Neural Coding of Whisker Timing in Multi-Whisker Sensation

Ching Fang

UC Berkeley Molecular & Cell Biology

Abstract

In order to examine the neural coding of complex stimuli in the mouse whisker system, we recorded neural spiking in the primary somatosensory cortex (S1) evoked by sequential deflections of various whisker pairs across a range of inter-whisker deflection intervals (IDIs). We constructed a population model by representing individual neurons as over-dispersed Poisson processes parameterized by IDI tuning curves. Using a population decoder, it was shown that the population could encode IDI information at a resolution of approximately 20 ms on a single-trial basis. We then determined a possible mechanism by which a population rate code could encode such information. Theoretically, neurons may convey the most information about stimuli at the point in the tuning curve where firing rate changes most steeply. Our results suggest instead that S1 neurons convey maximal information about whisker timing at their best IDI. Furthermore, most S1 neurons were spatially tuned for a specific whisker combination. The sharpest IDI tuning was found over each neurons preferred whisker combination, suggesting that receptive fields of the whisker system are space-time inseparable.

1. Introduction

Tactile sensation is complex, and how the nervous system encodes tactile input remains incompletely understood. The rodent whisker system provides a useful model for studying neural coding of touch. Rodents rely mainly on their whiskers to navigate and understand their environment. Natural whisker-based sensation relies on the rodent's ability to perceive complex spatiotemporal patterns of whisker deflections, making the whisker-to-barrel system a model of interest in studying sensory processing. Each whisker maps topographically to a unique cluster of neurons in a cylindrical region of the primary somatosensory cortex (S1). These are called whisker barrels. Collectively, these barrels make up the barrel cortex. Each of these barrels are greatly tuned to the stimulation of its associated facial whisker. The organization of major whiskers on the snout is identical to the organization of the barrels in the barrel cortex. Prior studies of whisker sensation mostly focused on how deflections or vibrations of single whiskers are encoded by S1 neurons. These studies have mapped many single-whisker features in the barrel cortex, such as direction of whisker deflection [1].

However, it is important to note that single whisker deflections are not reflective of natural stimuli that rodents experience. Natural whisker stimuli consists of complex spatiotemporal patterns of whisker deflection. How these are encoded is largely unknown, and not as deeply studied.

Most studies dedicated to complex stimulus encoding have focused on spatial identity of multi-whisker stimulation. Broadly speaking, many neurons in the barrel cortex are selective for global movement across whiskers in different directions and orientations. This selectivity must be a result of some nonlinear integration of responses across many whiskers [2]. More specifically, the response of some neurons to combined stimuli are can be smaller (supralinear) or greater (superlinear) than the sum of the response to each individual whisker, depending on location and other features [3]. Ramirez et al. discussed the idea of supra- and super- linearity with respect to adaptation. Since surrounding whiskers can facilitate and suppress responses to the principal whisker, neuron receptive fields can change under these conditions [4]. Adaptation can reduce the number of whiskers that a neuron responds to, effectively sharpening receptive fields [4]. Moreover, adaption may reduce supralinearity and linearize neuron responses to multi-whisker stimuli [4]. Furthermore, it has been shown that subpopulations of the barrel cortex are tuned to specific multi-whisker correlation patterns. Based on correlated versus uncorrelated multi-whisker stimuli, there appears to be a functional mapping in the rat barrel cortex [5]. An issue with studying these stimuli is that deflection patterns over many whiskers can give a combinatorially large stimulus space. However, responses to patterns of three-whisker deflections are predictable from responses to patterns of two-whisker deflections, indicating that studying the simpler structure of two-whisker deflections may be sufficient for studying complex whisker stimuli [6].

Other aspects of complex whisker stimuli besides whisker identity have been studied as well. Attention has also been given to the length of time between the movement of two whiskers, or the inter-stimuli interval (ISI). Facilitation and suppression occur at different time latencies and strengths depending on the location of the cells in the barrel cortex. Response facilitation is strongest for cells in the middle of the barrels given short ISIs, while response suppression is strongest for cells in between barrels [3, 7]. The role of facilitation in barrel cortex cells given shorter ISIs explain the ability of some cells to discriminate paired stimuli more accurately than single whisker stimuli [6]. Furthermore, cells may have preferential spiking for ISIs - some cells show greater temporal precision at ISIs consistent with the range of natural whisking frequencies [6].

We were interested in examining how timing was represented in the cortex. To this end, we delivered paired whisker stimuli to anesthetized mice while performing extracellular recordings in a barrel column, usually D1. Each paired stimulus consisted of the movement of a major facial whisker, and the movement of the anatomically correct columnar whisker (CW) of the column being recorded, and the movement of an adjacent surround whisker. For any paired stimulus, we delivered several trials of various inter-whisker deflection intervals (IDIs) from the range of -50 ms to 50 ms at a 1 ms resolution. This gives 101 possible IDIs in our data. Thus, a positive IDI of some time t_+ indicated stimulation of the CW precedes that of the surround whisker by t_+ milliseconds. Similarly, a negative IDI of some time t_- indicates stimulation of the CW followed that of the surround whisker by t_- milliseconds. We then used this data to construct a single-trial simulator of the S1 population response to various stimuli. Using this model and other analytical tools, we examined IDI coding in this neural population. We were particularly interested in seeing to what extent IDI was encoded in this population on the single-trial basis, and how this encoding varied across cortical layers.

We also wanted to examine possible IDI encoding mechanisms. Finally, we sought to test how spatial receptive fields interacted with temporal (IDI) receptive fields in this system.

2. Methods

2.1. Collection of Data

We recorded across layers 2-5 of the mouse barrel cortex using microelectrode arrays. Spiking data was collected from these recorded neurons in response to complex whisker stimuli. The stimuli in this data set consisted of a deflection of major facial whisker 5 and a deflection of one of its surrounding whiskers. Each pairing of whisker deflection is considered a whisker combination. Thus, given one major facial whisker, its eight surrounding whiskers, and two different phases of movement (in-phase or anti-phase), there were a total of 16 different whisker combinations possible. For each of these whisker combinations, we recorded trials over a range of IDIs from -50 ms to 50 ms, as described in the introduction.

2.2. Estimation of Tuning Curves

For each neuron, we then wanted to estimate the mean spiking response evoked for each IDI. As a noisy, first-order approximation of such an IDI tuning curve for a neuron, we merely took the average number of spikes evoked in response to each IDI. Since tuning curves are likely smooth over continuous stimuli, we then smoothed these noisy tuning curves using a Gaussian kernel, with kernel width chosen by cross-validation for each curve. Given n neurons and 16 possible whisker pair combinations, we thus had $16n$ unique curves total.

2.3. Filtering of Tuning Curves for IDI Significance

Of these $16n$ tuning curves, a large number were either effectively flat, or too noisy. Thus, it was of interest to us to isolate "significant" tuning curves that were likely modulated over IDIs, as opposed to tuning curves that were essentially flat and as such unmodulated over IDIs. To determine whether a smoothed tuning curve was significant or not, we ran the Benjamini-Hochberg procedure on the p-values associated with the Gaussian smoothing for that tuning curve. The tuning curves remaining from this procedure are considered IDI-significant, and collected into a set S. The neurons that contribute tuning curves to S comprise a set N_S, where $|N_S| < n$. We then ran principal component analysis on the normalized tuning curves of S to make generalizations about tuning curve shape. This was done through the `PCA` class of the `scikit-learn decomposition` package.

2.4. Creation of various population models

A basic model of a single neuron's response to a specific stimulus can be constructed as follows: given the estimated mean number of spikes evoked from that stimulus, μ, model the response output as some random variable X, where $X \sim Poiss(\mu)$. To incorporate the Fano factor, we estimate the variance σ of the neuron's response distribution to this stimulus. This gives the Fano factor $F = \frac{\sigma^2}{\mu}$. We arrive at a new model of the the response output as a random variable X', where $X' \sim NB(\mu, F\mu)$. This method of parameterizing the negative binomial distribution effectively models an over-dispersed Poisson point process [8]. Thus, to construct a population model over n neurons, we can make n such over-dispersed Poisson processes for each possible stimulus. To examine different aspects of temporal encoding, we created various population models using this paradigm:

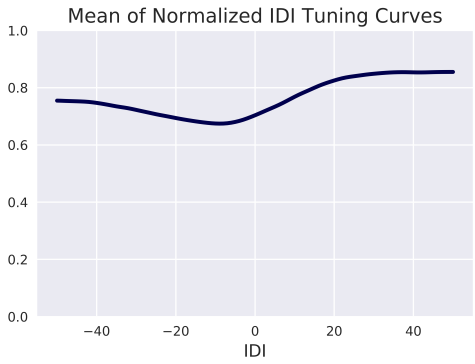

(a) PCA Mean

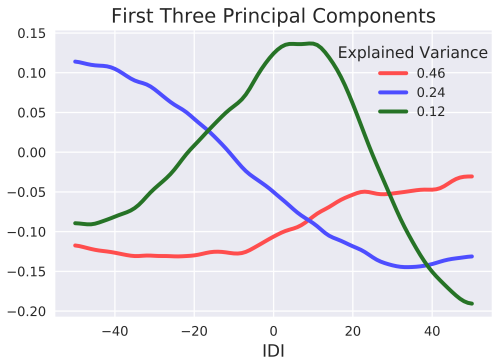

(b) PCA principal components

Figure 1: Results of PCA run on the normalized, significant IDI tuning curves

- `Standard Population`: This population contains n neurons, where each neuron responds according to its IDI tuning curve for a specific whisker combination.
- `Pooled Population`: This population contains $|S|$ "neurons". It is comprised of all significant tuning curves, with no distinction in response for different whisker populations. This allows us to examine temporal encoding over all spatial receptive fields.
- `Optimal Population`: This population contains $|N_S|$ neurons. It is comprised of all neurons in $|N_S|$, where each neuron responds to all stimuli with the IDI tuning curve corresponding to its optimal whisker combination. The IDI tuning curve of the optimal whisker combination is defined as the tuning curve where the max response of the curve for that whisker combination is larger than the max curve responses corresponding to other whisker combinations.
- `SubOptimal Population`: This population is the same as `Optimal Population`, except each neuron is defined by its second-best whisker combination.

2.5. Constructing a decoder over single-trial population responses

The decoder we used for any population with n neurons was a multinomial logistic regression model. The input to the model was $\vec{x} \in \mathbb{Z}_+^n$ where $\vec{x}_i$ is the spiking response of neuron i. The output of the model was a predicted IDI range, where the size of the range was r, a predetermined resolution size in milliseconds. The model was implemented with the `LogisticRegression` class of `scikit-learn`, using LASSO regularization, 7-fold cross validation, a multinomial loss function, and stochastic gradient descent. Train and test data was generated using the population models described above. Arbitrarily, we used 400 trials per class for testing data, and 1000 trials per class for training data.

2.6. Estimation of IDI resolution

It is possible to run the decoder over several different IDI range sizes. Thus, it is more accurate to estimate the resolution of the IDI encoding system and use that resolution for the decoder there on afterwards. First, we noted that the confusion matrices generated from the multinomial classification task gave a means of comparing how often two classes were

confused for each other. Two IDI classes that are often confused for each other are therefore likely to be within the real resolution range of the system. Thus, we generated a confusion matrix for an arbitrarily small IDI range size of 5 ms. This size is physiologically unlikely to be the real resolution size, and provides a way of measuring the change in confusion over different possible resolutions. To that end, we plotted the mean confusion as a function of t, where t indicates a comparison between classification of an IDI of 0 ms and classification of an IDI of t milliseconds (Fi). By examining this plot, we found that the system likely had an IDI encoding resolution of 20 ms.

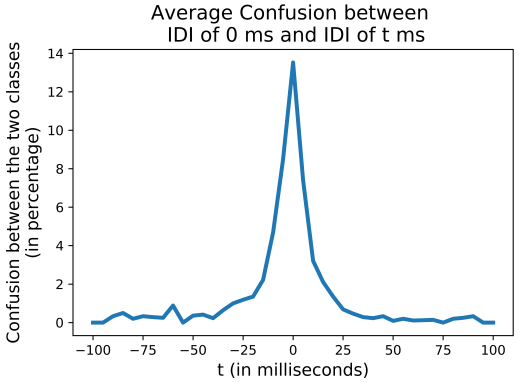

Figure 2: Change in confusion as a function of resolution

2.7. Comparison of IDI tuning across different cortical layers

Comparison of decoding accuracy was done through one-way ANOVA, with Tukey's range range test post-hoc.

3. Results

We used a combination of the neural population model and a decoder to demonstrate the extent in which IDI's are encoded by the population, as well as other mechanisms and details of this system with respect to IDI encoding.

3.1. Testing whether IDI is encoded by the population

By examining the main three principal components of the IDI tuning curves in S, we can see that IDI encoding can be inferred on average. The main three principal components together capture 82% of the variance over these tuning curves (Figure 1b). The first two principal components indicate a sigmoidal shape in the tuning of individual neurons for IDIs (Figure 1b). On the single trial response basis, we found that the decoder could predict IDIs well above chance probability just from the raw data. This can be seen upon examination of Figure 3, where the diagonal values of the confusion matrix are greater than the predicted values of chance decoding performance (20%). Using tuning curve estimation to parameterize `Standard Population` and `Pooled Population`, we obtain an accuracy rate of around 80% using the estimated resolution range of 20 milliseconds (Figure 4).

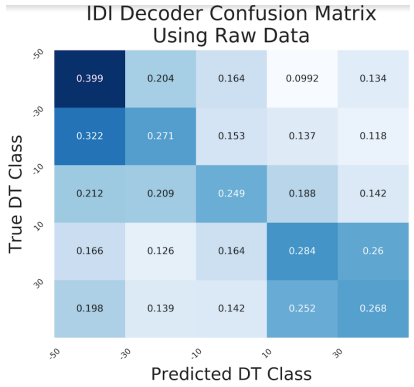

Figure 3: Accuracy of IDI Decoder using Raw Data (no models)

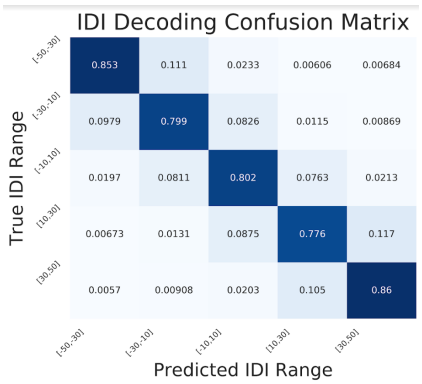

(a) Decoder accuracy using `Pooled Population`

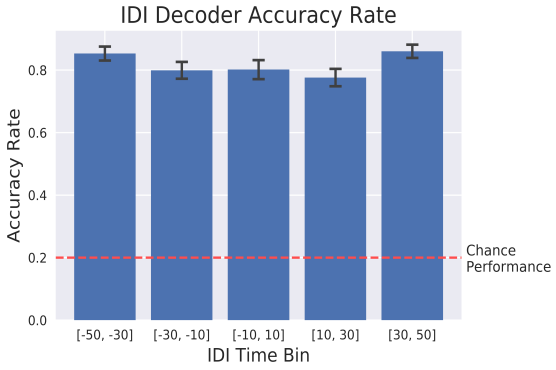

(b) Decoder accuracy using `Pooled Population`, with standard deviations shown

Figure 4: Accuracy of IDI Decoder

3.2. Examining trained decoder

There are two possible theories for describing where the maximal information of a neuron is encoded: the slope of its tuning curve, or the peak of its tuning curve. In other words, for IDI decoding, the population may be relying on a basis of sigmoidal tuning curves, or a basis of "peaked" tuning curves. Two examine these two ideas, for any neuron with length 101 tuning curve $\vec{c}$ where $\vec{c}_i$ gives the average spiking response to the ith possible IDI, we defined two terms:

$$t_{max} = \arg\max_i \vec{c}_i$$

$$t_{center} = \arg\max_i |\overline{c_{[1,i]}} - \overline{c_{[i,101]}}|$$

. In other words, the t_{max} of any tuning curve represents the IDI that would elicit the maximal response. The t_{center} of any tuning curve represents the IDI

Next, we note that, for 5 possible IDI ranges, the logistic regression decoder assigned each neuron a specific weight for each IDI range. Thus, for each IDI range, it was possible to inspect which neurons were positively weighted by the logistic regression model. Thus, a possible interpretation is that the increased activity of these positively-weighted neurons would indicate the occurrence of their associated IDI range. We examined the distribution

of each neuron's t_{max} and t_{center} values for the positively-weighted neurons of each class. We found that the t_{max} distributions for each class formed a largely disjoint basis over the IDI axis (Figure 5a) In contrast, the t_{center} distributions of each class overlapped significantly and did not form a clear disjoint basis (Figure 5b).

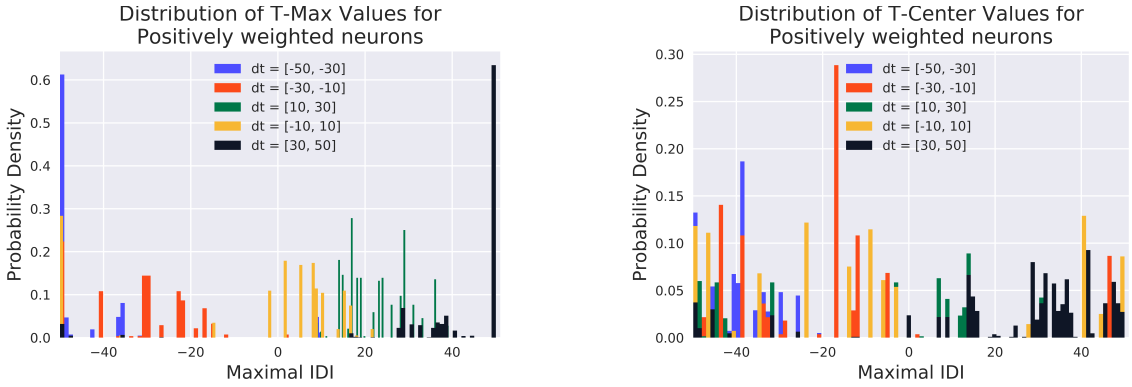

(a) (b)

Figure 5: Comparison of t_{max} and t_{center} distributions

3.3. Comparing temporal receptive fields with spatial receptive fields

To see if IDI decoding accuracy was different between a neuron's optimal 2-whisker combination versus a neuron's suboptimal 2-whisker coombination, we compared the decoder accuracy of `Optimal Population` to that of `Suboptimal Population`. We found that temporal decoding accuracy rate was higher over a population defined over the optimal 2-whisker combination of the neurons as opposed to the suboptimal 2-whisker combination (Figure 6).

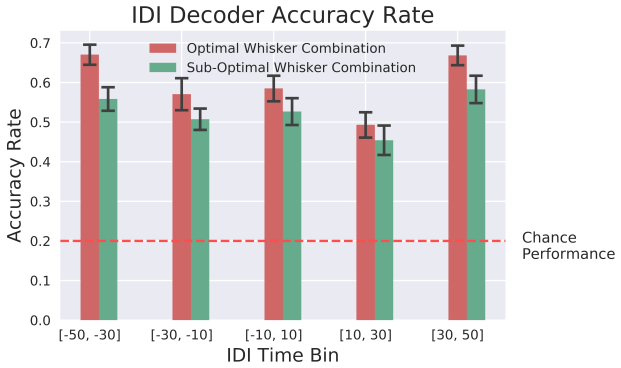

Figure 6: IDI decoding accuracy over different spatial receptive fields

3.4. Comparing IDI decoding performance over different cortical layers

For all neurons in `Pooled Population`, we separated neurons by the layer in which they were recorded, so that we had `Layer 2/3 Population`, `Layer 4 Population`, and `Layer 5 Population`. For each layer-specific population, we wanted to examine how IDI decoding accuracy changed over different IDI ranges. First, for each layer we generated boxplots

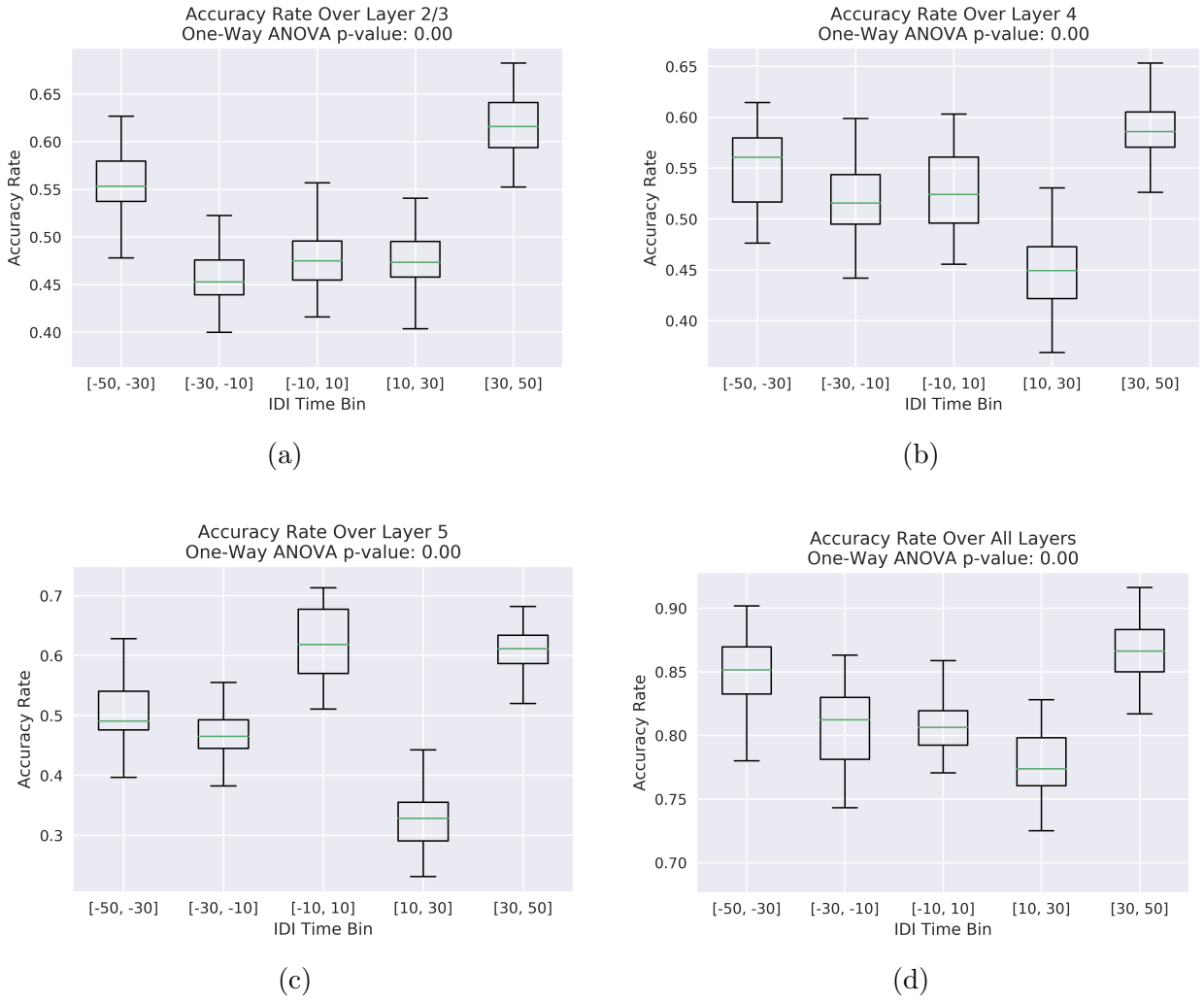

Figure 7: Boxplots of IDI encoding accuracy over different layers

of the accuracy rates over the IDI ranges. From this, we can speculate, for instance, that layer 2/3 may be preferentially tuned to longer IDIs. We then ran a one-way ANOVA using the `scipy.stats` module. We could significantly reject the one-way ANOVA for all layers; however, this does not not mean there is a clear pattern in IDI encoding across layers, as we can only conclude that encoding accuracy changes over different IDI ranges in general.

More specifically, we wanted to see if certain layers had preferential encoding for particular types of IDIs (e.g., short versus long, positive versus negative). For each neuron population of a specific layer, we used Tukey's range test (implemented through Python's `statsmodel` multiple comparisons library) to the set of all pairwise comparisons between accuracy rates in decoding different IDI bins. However, for all layers, each IDI range was classified as its own unique class under Tukey's test. Furthermore, the boxplots show physiological inconsistency across the IDI axis; it is unlikely in layer 4 that encoding accuracy would suddenly drop only for IDIs in the range of 10 to 30 ms. Overall, no conclusions could be drawn about patterns of IDI encoding over the different layers.

4. Discussion

From our results, we can see that IDI is encoded by the population on the single trial basis, with an estimated resolution of 20 milliseconds. We then tried to characterize the functional role of tuning curves in this population. In theory, it is possible for neurons to encode stimuli at the tuning curve peak, or at the high-slope regions of the tuning curve [9]. The clear disjoint segmentation we saw of the IDI axis by t_{max} distributions suggest that S1 neurons convey maximal information about whisker timing at the peak of their tuning curves, as opposed to the steeply sloped regions of their tuning curves. However, these findings may be a reflection of neuronal variability or effective population size. Greater response noise in the measured population may contribute to maximum-firing-rate encoding playing a greater role in stimulus discrimination [9]. Thus, although maximal-firing-rate encoding may be the encoding mechanism used by these neurons, our experimental methods may be a contributing factor to this. For instance, because of the large number of stimuli possibilities, the number of trials for each individual IDI was fairly low. This means high variability of neuron response may be a result of estimation error.

Since IDI tuning is more accurate at any neuron's optimal whisker combination than at some suboptimal whisker combination, this indicates that temporal receptive fields are inseparable from spatial receptive fields in the whisker system. Interestingly, there seems to be stronger temporal tuning where spatial tuning is the greatest. This could indicate a more sparse method of encoding in this system. A neuron needs only to be responsible for IDI tuning at its preferred whisker combination, instead of over all possible whisker combinations. Gaining a greater insight into how complex spatiotemporal stimulation patterns can elucidate how natural stimuli are encoded. Rodents are capable of discriminating different textures with great efficacy, yet the exact features that neurons use to discriminate between rough and smooth textures are not obvious [10]. However, one can imagine that, while a mouse whisks rostro-caudally over a stationary object of some unknown texture, the IDI between two adjacent whiskers is related to the object texture. A more textured object would result in a greater delay between one whisker brushing a "bump" in the object surface and the second whisker brushing another "bump" in the object surface. A more smoothly textured object could thus be related to a smaller IDI. Similarly, IDIs across different rows of whiskers can be related to global motion and object orientation as described by Jacob et al [2]. For example, a diagonally oriented object would result in greater IDIs between whiskers on the same row, as opposed to the near-0 IDI elicited by a horizontally oriented object.

IDI coding can also provide information about moving objects. The IDI between two whiskers can be used to infer the velocity of some moving object. For instance, two mice moving past each other in a tunnel can use their whiskers to sense the movement velocity of the other; here, a greater velocity would correspond to a shorter IDI. Thus, we have found more information on how IDIs are encoded in this system, as well as their relation to spatial receptive fields; this gives a clue as to how more complex natural stimuli are encoded in the brain.

In future studies, it would be of interest to examine other features of complex whisker stimuli. To see how relatively simpler features of paired whisker identity and IDIs gener-

alize over different whisker sensations, we could also examine how responses to much more complex sensations can be predicted from simpler features. Furthermore, examining how different receptive fields for different features interact would give greater insight to how the whisker system processes information, and perhaps how computation across layers change. Since complex whisker stimuli tends to be high dimensional, a greater number of recordings would be necessary to ensure data is not sparse, and that more details of whisker encoding can be directly estimated from the data.

5. References

[1] C. C. Peterson, The functional organization of the barrel cortex, Neuron 56 (2007) 339–355.

[2] V. Jacob, J. Le Cam, V. Ego-Stengel, D. E. Schulz, Emergent properties of tactile scenes selectively activate barrel cortex neurons, Neuron 60 (2008) 1112–1125.

[3] S. Shimegi, T. Akasaki, T. Ichikawa, H. Sato, Physiological and anatomical organization of multiwhisker response interactions in the barrel cortex of rats, The Journal of Neuroscience (2000).

[4] A. Ramirez, E. A. Pnevmatikakis, J. Merel, L. Paninski, K. D. Miller, R. M. Bruno, Spatiotemporal receptive fields of barrel cortex revealed by reverse correlation of synaptic input, Nature Neuroscience 17 (2014).

[5] L. Estebanez, J. Bertherat, D. Schulz, L. Bourdieu, J. Leger, A radial map of multiwhisker correlation selectivity in the rat barrel cortex, Nature Communications (2016).

[6] A.-R. Boloori, G. B. Stanley, The dynamics of spatiotemporal response integration in the somatosensory cortex of the vibrissa system, The Journal of Neuroscience (2006).

[7] V. Ego-Stengel, T. M. E. Souza, V. Jacob, D. E. Schulz, Spatiotemporal characteristics of neuronal sensory integration in the barrel cortex of the rat, Journal of Neurophysiology 93 (2004).

[8] G. Rodriguez, Lecture notes on generalized linear models, 2007.

[9] D. A. Butts, M. S. Goldman, Tuning curves, neuronal variability, and sensory coding, PLOS Biology 4 (2006).

[10] T. Prigg, D. Goldreich, G. E. Carvell, D. J. Simons, Texture discrimination and unit recordings in the rat whisker/barrel system, Elsevier Science (2002).